ISSN 0006-2979, Biochemistry (Moscow), 2024, Vol. 89, No. 5, pp. 942-957 © Pleiades Publishing, Ltd., 2024.

# *In vitro* and *in vivo* Evaluation of Antifibrotic Properties of Verteporfin in a Composition of a Collagen Scaffold

**Olga S. Rogovaya[1,a]*, Danila S. Abolin[1], Olga L. Cherkashina[1], Artem D. Smyslov[1], Ekaterina A. Vorotelyak[1], and Ekaterina P. Kalabusheva[1]**

[1]*Koltzov Institute of Developmental Biology, Russian Academy of Sciences, 119334 Moscow, Russia*
[a]*e-mail: rogovaya26f@yandex.ru*

Received December 6, 2023
Revised March 5, 2024
Accepted March 31, 2024

**Abstract**—Extensive skin damage requires specialized therapy that stimulates regeneration processes without scarring. The possibility of using combination of a collagen gel application as a wound dressing and fibroblast attractant with verteporfin as an antifibrotic agent was examined *in vivo* and *in vitro*. *In vitro* effects of verteporfin on viability and myofibroblast markers expression were evaluated using fibroblasts isolated from human scar tissue. *In vivo* the collagen gel and verteporfin (individually and in combination) were applied into the wound to investigate scarring during skin regeneration: deviations in skin layer thickness, collagen synthesis, and extracellular matrix fibers were characterized. The results indicate that verteporfin reduces fibrotic phenotype by suppressing expression of the contractile protein Sm22α without inducing cell death. However, administration of verteporfin in combination with the collagen gel disrupts its ability to direct wound healing in a scarless manner, which may be related to incompatibility of the mechanisms by which collagen and verteporfin control regeneration.

**DOI**: 10.1134/S0006297924050146

*Keywords*: dermal fibroblasts, fibrosis, skin regeneration, verteporfin, YAP/TAZ

## INTRODUCTION

Wound healing is a complex process, which is commonly considered to be divided into sequential partly overlapping four phases: hemostasis, inflammation, proliferation (cell infiltration, angiogenesis, and re-epithelialization), and maturation/remodelling [1]. At the phase of inflammation activation of immune cells stimulates secretion of cytokines, which, in turn, activate migration of fibroblasts, epithelial and endothelial cells to the damaged area. In the wound bed fibroblasts acquire activated phenotype and are transformed into Sm22 positive myofibroblasts, which are cells responsible for generation of main components of extracellular matrix such as fibronectin with extra domain A, collagen I and III, required for filling-in defects of connective tissues and scar formation [2-4]. Remodelling phase is the final phase of wound healing, which could take years. At this stage under normal conditions architecture of the restored tissue is close to the structure of normal skin [1].

When the damage is very extensive, specialized agents are used to stimulate regeneration process. Tissue equivalents based on the collagen gel are successfully introduced into the medicine practice [5]. Biodegradability of collagen and its low immunogenicity make it an optimal base not only for tissue engineering involving design of constructs containing collagen-based scaffolds and live cells, but also for developing collagen-based wound dressings [6-8]. Collagen, as a key element of extracellular matrix, affects all stages of wound healing [9-11]. Collagen hydrogels partially reproduce properties of extracellular matrix, have porous structure with a network of protofibrils enabling migration and colonization of cells, thus facilitating remodelling of the *de novo* formed tissue and wound healing [12]. In some cases, the collagen-based

*Abbreviations*: BrdU, 5-bromo-2′-deoxyuridine; BSA, bovine serum albumin; DPBS, Dulbecco's phosphate-buffered saline; PFA, paraformaldehyde; VP, verteporfin.

* To whom correspondence should be addressed.

skin substitutes contain biologically active molecules: growth factors, cytokines or their analogues that stimulate the processes of integration of the tissue equivalent into the damaged organ, regeneration of the adjacent tissues, and modulation of immune response.

One of the often complications of skin regeneration, especially in the cases of extensive damages such as burns requiring specialized therapy, is formation of hypertrophic scars [13]. In addition to obvious cosmetic issues, scars disrupt mechanical interactions in the skin making it more fragile and prone to rapture. Scars do not contain hair follicles and accompanying sebaceous glands, which promotes drying of epidermis. One of the newest and most promising therapeutic preparations for anti-scar therapy is verteporfin (VP) [14-17].

Single administration of VP to mice at the early stages of regeneration initiated the process of scarless healing [18]. VP also exhibits bactericidal activity, which produces beneficial effects on would healing [16]. Delivery of VP to the damage area for stimulation of wound healing was successfully performed using agents based on fibroin [15], polyvinyl [17], and polylactide [14]. We investigated the possibility of using collagen gel as a VP delivery agent to the wound, in order to prevent scar formation after complete wound healing.

The anti-scar properties of VP are considered to be associated with its ability to inhibit interaction of the transcription cofactor YAP1 with its targets from the family of TEAD proteins. Activation of the YAP1 signaling cascades occurs during wound healing both in epidermis and in dermis [19]. In epidermis it stimulates migration and proliferation of keratinocytes in the wound bed. Active nuclear YAP1 is associated with proliferation of fibroblasts and increase of their contractile ability, which is important for wound closing. Activity of this signaling cascade decreases at the stage of remodeling. Increase of the duration of activity of the YAP1 signaling cascade in mice results in formation of common or hypertrophic scars, at the same time, its inhibition in fibroblasts at the early stages of wound healing stimulates regeneration of a fully functional skin with all derivates [20].

Effect of VP on scarring processes were examined both *in vitro* and *in vivo*. For the *in vitro* studies human fibroblasts isolated from hypertrophic skin scar were applied as an analogue of myofibroblasts of the wound bed. Effect of VP on viability, expression of contractile markers, and contractile ability of fibroblasts were examined. In the *in vivo* studies with laboratory mice, efficiency of VP administration in composition of collagen gel for stimulation of skin regeneration was investigated. The following parameters were analyzed: rate of the wound closure, structure of extracellular matrix, and general morphology of the regenerated skin.

## MATERIALS AND METHODS

**Isolation and cultivation of dermal fibroblasts.** Cells lines used in the study were isolated from human skin biopsies obtained in the course of reconstructing surgeries in the Vishnevsky National Medical Research Center for Higher Technologies with informed consent of the donors. Experiments with skin biopsies were performed in accordance with the protocol approved by the Bioethics Committee of the Koltzov Institute of Developmental Biology, Russian Academy of Sciences (IDB) (no. 51 from 09.09.2021). Biopsy samples were washed with a Hank's solution (PanEco, Russia) supplemented with 0.4 mg/ml of gentamycin (BioFarmGarant, Russia) for disinfection, next, subcutaneous fat and reticular layer of dermis were removed mechanically in such a way that the upper layer of skin with epidermis was no thicker than 2 mm. Dermis with epidermis were cut into 2-3 mm bands and incubated in a 2% Dispase solution (Gibco, USA) for 1 h at 37°C; in the next step epidermis was removed, dermis was cut by scissors to homogenous state and incubated in 0.1% collagenase type I solution (Gibco) for 24 h at 37°C. The obtained mass was centrifuged at 140*g* for 10 min, precipitate was resuspended in a DPBS (Dulbecco's phosphate-buffered saline; PanEco); this procedure was repeated three times.

To isolate scar fibroblasts normal tissues were removed from the biopsy sample, only regions with pronounced scarring deformation were preserved, which was followed by incubation of the sample for 1 h in a 2% Dispase solution at 37°C. After removal of epidermis, dermis was cut with scissors to homogenous state and incubated in a 0.1% Liberase solution (Roche, USA) for 24 h at 37°C. The obtained sample was centrifuged at 140*g* for 10 min; precipitate was resuspended in DPBS; procedure was repeated 3 times.

Isolated fibroblasts were cultivated in 25 $cm^2$ culture flasks an Amniomax-II medium (Gibco) under conditions of 5% $CO_2$ and 37°C. Culture medium was replaced every 2-3 days. After reaching confluency, cells were detached using a 0.05% trypsin-EDTA solution (Capricorn, Germany) followed by cultivation in a DMEM medium (PanEco) supplemented with 10% fetal bovine serum (Capricorn), 1% Glutamax (Cibco), 1% penicillin-streptomycin (Gibco). Cells after 2-3 passages were used in the study.

Samples of a healthy skin obtained from three 42-55 years old donors, and samples obtained from the 33-45 years old donors with scar tissues were used in the study. Produced cell lines were deposited to the IDB collection of cell lines for biotechnological and biomedical studies (general biology and biomedical section).

**Detection of apoptosis.** In order to determine type of the cell death, fibroblasts were detached from

**Table 1.** Sequences of primers used in the study

| Gene name | Forward primer | Reverse primer |
|---|---|---|
| *GAPDH* | CCATGTTCGTCATGGGTGTG | GGTGCTAAGCAGTTGGTGGTG |
| *HPRT* | ACCAGGTTATGACCTTGATT | AAGTTGGCCTAGTTTATGTT |
| *YAP* | AGAGAATCAGTCAGAGTGCTCCA | TTCAGCCGCAGCCTCTCC |
| *TAZ* | GGCAATGATTAAACTGGCAACA | AGTGAGCCCTTTCTAACCTGG |
| *CTGF* | TGTGCACCGCCAAAGATG | CAGACGAACGTCCATGCTG |
| *CYR61* | AAGGAGGCCGTCCTGGTC | GGGCTGCATTCCTCTGTGT |
| *EDA-FN* | CCCTAAAGGACTGGCATTCA | CATCCTCAGGGCTCGAGTAG |
| *CD26* | AGAAGGAGTATTCAATAAGTGGGAC | TACTCTGCTCTGTGGTGGTCT |
| *COL1* | AGAAAGGGGTCTCCATGGTG | AGGACCTCGGCTTCCAATAG |
| *COL3* | CCAGGAGCTAACGGTCTCAG | TGATCCAGGGTTTCCATCTC |

the surface 1, 3, and 5 days after treatment with VP, centrifuged at 140*g* for 5 min, washed once with DPBS, followed by incubation for 15 min in a solution of annexin V and propidium iodide using an apoptosis detection kit PI-AV (BD Pharmingen™, USA) according to manufacturer instructions. To introduce compensation coefficient to the results of analysis, samples stained separately with annexin V and propidium iodide were used. Flowcytometry analysis was carried out with an Attune® NxT flow cytometer (Life Technologies, USA).

**Cultivation of fibroblasts in a collagen gel.** To prepare gel, a 0.34 M NaOH solution (Khimmed, Russia) – 6.5%; 7.5% $Na_2CO_3$ solution (PanEco) – 3.42%; 10× M199 medium (Gibco) – 9.77%; Glutamax (Gibco) – 0.39%; Hepes (PanEco) – 1.95% collagen type I solution – 77,97% were mixed on ice. Collagen solution was prepared from the standard laboratory rat tail tendons: individual fibers were separated mechanically and dissolved in a 0.1% acetic acid, final concentration – 2 μg/ml. Gel aliquots (400 μl) containing cell suspension (150 × $10^3$ cells per ml) were inoculated into wells of 24-well plate (Corning, USA) and incubated at 37°C for polymerization. Culture medium (500 μl) was added on top of the gel. Gel was separated from the culture well walls, which facilitated unlimited contraction of the gel by cells.

One day after the gel formation, VP (Sigma-Aldrich) solution in a culture medium at concentration 0.1 μg/ml was added to experimental wells followed by incubation with the cells for 24 h followed by washing the gel once with a Hank's solution and immersing the gel into a regular culture medium.

**Quantitative PCR analysis.** RNA was isolated with the help of a RNAzol reagent (Sigma-Aldrich, Germany) according to the manufacturer's instructions. A QuantiTect Reverse Transcription Kit (Qiagen, USA) was used for genomic DNA removal and performing reverse transcription. One μg of RNA was used for reverse transcription reaction. Real-time quantitative PCR was carried out using a 5× qPCRmix-HS SYBR+LowROX reagent kit (Evrogen, Russia) and a LightCycler96 amplifier (Roche). Reaction protocol: 10 min at 95°C, 1 cycle; next 45 cycles including 20 s at 95°C, 20 s at 60°C, 30 s at 72°C. All experiments were performed in three biological and technical replicates. Amount of product in each sample was calculated using the $2^{-\Delta\Delta Cq}$ method and normalized to expression of GAPDH and HPRT. Data on the graphs are presented as mean ± standard deviation. Sequences of the primers used in the study are presented in Table 1.

**Incorporation of BrdU label and determination of the cell cycle stage.** Fibroblasts (500 × $10^3$ cells) were seeded into 25 $cm^2$ culture flasks (Corning) and cultured for 1 day. Next, VP was added at concentration 0.1 μg/ml. Concentration of VP was determined previously (unpublished data) with consideration of the literature data [18] and cultivation was continued for 1 day followed by removal of VP with replacing culture medium. Next, a BrdU label (5-bromo-2′-deoxyuridine; Sigma-Aldrich) was introduced on the day 1, 3, and 5 of cultivation to final concentration 30 μM followed by 2-h incubation. Cells were detached, washed with DPBS, and fixed in a 70% ethanol solution for 1 h at 4°C. Next cell was precipitated by centrifugation for

**Table 2.** Antibodies used in the study

| Antibodies | Manufacturer, cat. no. | Dilution | Fluorophore |
|---|---|---|---|
| Primary anti-BrdU rat IgG | Abcam, ab6326 | 1/100 | – |
| Primary goat IgG against Sm22α | Abcam, ab10135 | 1/100 | – |
| Primary rabbit IgG against YAP1 | Abcam, ab52771 | 1/100 | – |
| Primary rabbit IgG against YAP1 | Cell Signaling Technology, D8H1X | 1/100 | – |
| Primary rabbit IgG against collagen I + III | Imtek (Russia), RAP c13 | 1/20 | – |
| Primary goat IgG against P-cadherin | R&D Systems, AF761 | 1/20 | – |
| Primary rat IgG against E-cadherin | Abcam, ab11512 | 1/20 | – |
| Secondary donkey IgG against rabbit IgG | Invitrogen, 32790 | 1/1000 | Alexa 488 |
| Secondary donkey IgG against goat IgG | Life Technologies, A11056 | 1/1000 | Alexa 546 |
| Secondary goat IgG goat against rat IgG | Life Technologies, A11081 | 1/1000 | Alexa 546 |

2 min at 1000*g*; 0.5 ml of 2 M HCl (Khimreaktiv, Russia) containing 0.5% Triton X-100 (MP Biomedicals, USA) was added to the precipitate and incubated for 30 min at room temperature. Cell was precipitated, supernatant was removed, and cells were resuspended in 0.5 ml of 0.1 M sodium tetraborate (Khimmed, Russia). The mixture was incubated for 2 min and, next, washed once with 150 µl of DPBS/1% BSA (bovine serum albumin; PAA, Austria), and next incubated with 50 µl of a primary antibody solution in DPBS with addition 0.5% Tween 20 (MP Biomedicals) and 1% BSA for 1 h at room temperature. Cells were washed once with DPBS and incubated in a solution of secondary antibodies for 30 min at room temperature (manufacturers and dilutions of antibodies are presented in Table 2). Next, cells were resuspended in 0.5 ml of DPBS containing 10 µg/ml of RNAse A (Fermentas, Canada) and 20 µg/ml of propidium iodide solution (Sigma-Aldrich) followed by 30-min incubation in the dark. Cells stained with relevant secondary antibodies and non-stained cells were used as controls. Flow cytometry was carried out using an Attune® NxT flow cytometer.

**Immunofluorescent staining of collagen gels.** Gels were fixed with a 4% solution of paraformaldehyde (PFA) (Sigma-Aldrich) for 40 min, washed once with DPBS, and permeabilized in a DPBS solution containing 1% Tween 20, 1% Triton X-100, and 5% BSA for 1 h at room temperature. Next, primary antibodies at concentrations shown in Table 2 were added and incubated for 12 h at 4°C. Next, the samples were washed with permeabilizing solution for 2 h followed by addition of the corresponding secondary antibodies conjugated with fluorophores (Table 2) and 12-h incubation at 4°C. Nuclei were stained with DAPI (Biotium, USA) at concentration 1 µg/ml. Imaging and image analysis was carried out with the help of an Olympus IX 73 fluorescence microscope (Olympus, Japan).

**Surgical procedures.** Male C57Bl6 mice ($n$ = 24) at the age of 8 weeks were used in the study. All experiments were conducted with animal under general anesthesia in accordance with the International Guiding Principles for Biomedical Research Involving Animals [21, 22]. Animal were kept with free access to water and feed.

Mice were divided into the following groups: Control ($n$ = 6), VP ($n$ = 6), Gel ($n$ = 6), and Gel + VP ($n$ = 6). Animals were anesthetized with isoflurane VetFarm, Russia). Hair was shaved between the shoulder blades, and surgical area was disinfected with 70% alcohol. Ketoprofen solution (50 mg/ml, Ellara, Russia) was injected into a surgical area. A 5-mm diameter circle was cut from all layers of the skin. To prevent rapid contraction, a silicone ring (splint) with diameter corresponding to the wound size was applied, the ring was glued with a BF-6 glue (Tulskaya Farmatsevticheskaya Fabrika, Russia) and fixed in place with 8 surgical stiches using a nonabsorbable suture (Resolon, Germany). The wound was rinsed and 250 µl of collagen gel ('Gel' group), 100 µl of VP solution in PBS with concentration 1 mg/ml ('VP' group), or 250 µl of collagen gel with VP ('Gel + VP' group at the rate 100 µg of VP per mouse) were administered into the wound of animals in experimental groups. In the 'Control' group 100 µl of PBS solution with added DMSO (dilution 1/1) was

applied to the wound. Wounds were covered with a Tagaderm film (3M, Germany) and fixed with a bandage (Omniplast, Germany).

Collagen gel for introduction into wounds was prepared the same way as in the case of fibroblast cultivation. Gel (250 μl) was placed into the wells of a 48-well plate (Corning) and incubated at 37°C for polymerization.

State of wounds in animals was examined every other day, and additional sutures were applied to the silicon rings if required. Wounds were photographed once a week.

All abovementioned agents were introduced once more into the wounds after 3 days. On the day 21 of the experiment the animals were euthanized, post-mortem 7-8 mm diameter biopsy samples including entire skin thickness were taken from the wounds.

**Handling of wound biopsy samples and histological staining.** Wound biopsies were embedded into a Tissue-Tek medium (Sakura, Japan) forming cryoblocks by incubation first in nitrogen vapour and, next, immersing them into liquid nitrogen several times for 3-5 s until completely frozen; samples were stored at –70°C. Cryosections of the samples with 8 μm thickness were prepared with a Leica CM1950 cryostat (Leica, Germany).

Sections were fixed in a 4% PFA solution, stained with a hematoxylin-eosin stain (BioVitrum, Russia) according to the manufacturer's protocol, and embedded into a Bio Mount medium (BioOptica, Italy). Imaging of the stained samples was carried out with a Keyence BZ-9000 microscope (Keyence, Japan).

For immunofluorescence analysis, sections were fixed in a 4% PFA solution, incubated in a solution of primary antibodies containing 5% BSA, 1% Triton X-100, and 1% Tween 20 for 18 h, primary antibodies were next removed by washing in DPBS, and incubated with solution of secondary antibodies for 1.5 h. Imaging of the samples was carried out with a Leica Thunder microscope (Leica). List of the antibodies and their concentration are shown in Table 2.

**Analysis of collagen fibers architecture.** Architecture of collagen fibers was analyzed in the samples stained with hematoxylin-eosin. Dermis in the wound area was imaged with 40× magnification, the obtained images were analyzed with the help of CurveAlign and CT-FIRE algorithms [23, 24].

The CurveAlign algorithm analyzes the degree of alignment of collagen fibers in an image and constructs heat map of the fiber orientation; CT-FIRE uses curvelet transformation to suppress noise in the image and determine boundaries of collagen fibers, and, next, extracts information and analyzes parameters of individual collagen fibers (length, width, straightness, angle) [23, 24]. The obtained data were statistically processed.

**Statistical analysis.** Statistical data processing was carried out with the help GraphPad Prism 9 program. Prior to selection of statistical criterium each data set was analyzed for normality of distribution (Shapiro–Wilk test, Kolmogorov–Smirnov test, D'Agostino–Pearson combined test, Anderson–Darling test). In the case of normal data distribution differences between groups were analyzed with the help of one-way analysis of variance (ANOVA) with *post hoc* Tukey test for multiple comparisons, or with the help of two-way ANOVA supplemented with the Sidak test for pairwise comparisons. In the case of deviation from normal distribution differences between the data were analyzed with the Kruskal–Wallis test and *post hoc* Dunn's test for multiple comparisons. Presence of outliners in the data was determined with the help of Dixon's Q test.

The data obtained with the help of algorithms for analysis of collagen fiber architecture were processes using the OriginPro 2022 software. Principal component analysis was performed based on the results obtained with the help of these algorithms. The graphs show 95% confidence intervals for each group of data. K-means clustering was performed to identify similar data sets.

## RESULTS

**Effect of VP on viability of normal and scar-derived fibroblasts.** At the first stage of the study, we evaluated effect of VP on viability of normal and scar-derived human skin fibroblasts. For this purpose, the cell cultures were treated with VP solution for 24 h and, next, number of live and dying cells was determined with the help of propidium iodide and annexin V staining after 1, 3, and 5 days of cultivation (Fig. 1, a and b). Live cells were identified based on lack of staining with propidium iodide and annexin V. The level of proliferation was determined based on the number of cells with incorporated BrdU (Fig. 1c).

No statistically significant changes in the number of live/dying cells after treatment with VP were observed. However, treatment with VP significantly decreased proliferation in the normal and scar-derived fibroblasts one day after treatment. Three days after treatment the levels of proliferation between the control (norm and scar) and experimental groups (norm + VP, scar + VP) groups differed not very significantly, but the decreasing trend was observed. On the fifth day after treatment the scar-derived fibroblasts exhibited tendency for increased level of proliferation in the 'VP' group in comparison with the control group. Interestingly enough, proliferation decreased in the groups not treated with VP from day 1 to 5. This is associated with the contact inhibition in the course of reaching the confluence.

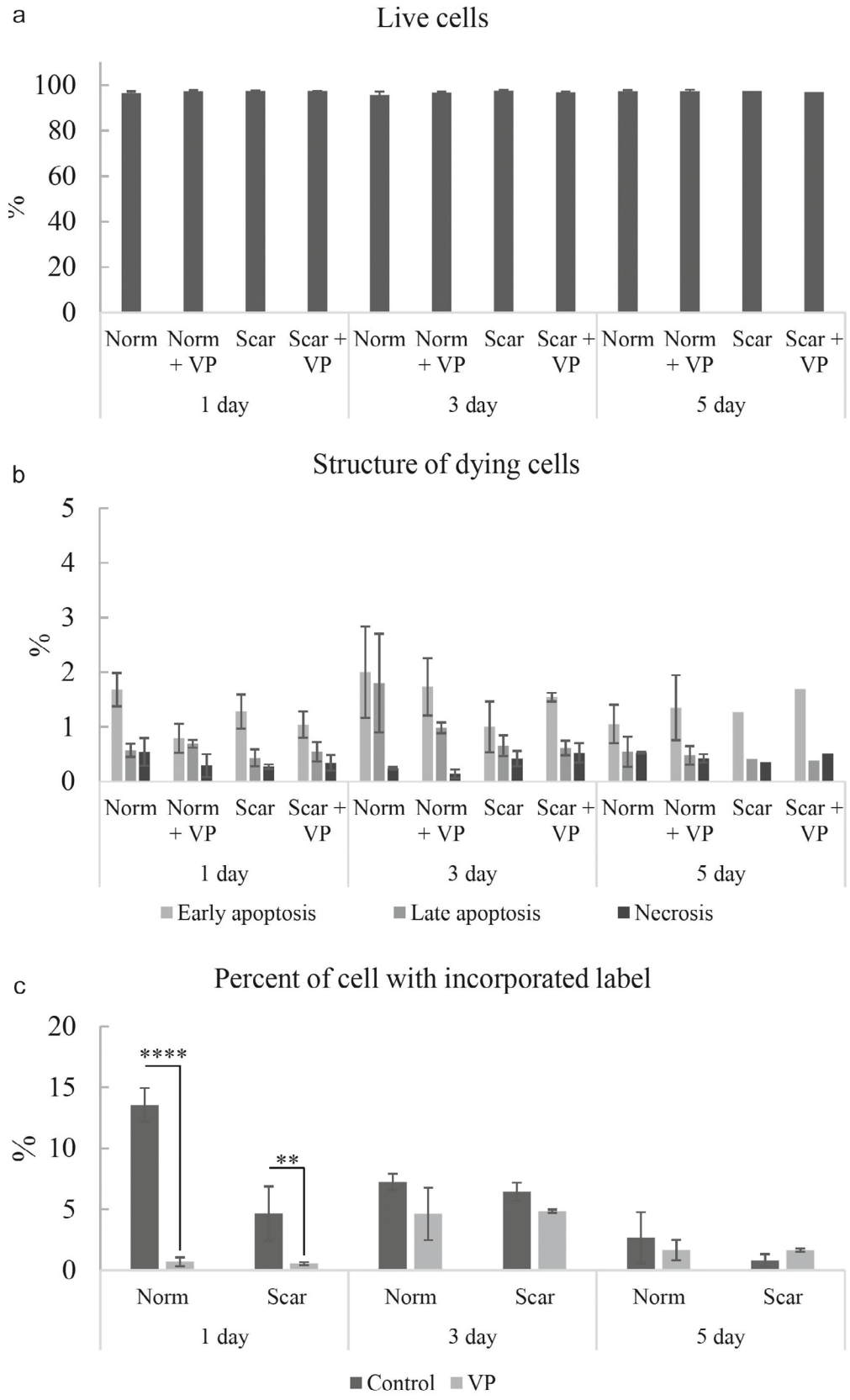


**Fig. 1.** Evaluation of the number of dead and proliferating fibroblasts of different types (norm and scar) under the action of VP. a) Fraction of live cells after treatment with VP. b) Fraction of dying cells after treatment with VP. c) Number of proliferating cells. Data are presented as a mean ± standard deviation. Statistically significant differences: ** $p \leq 0.01$ and **** $p \leq 0.0001$.

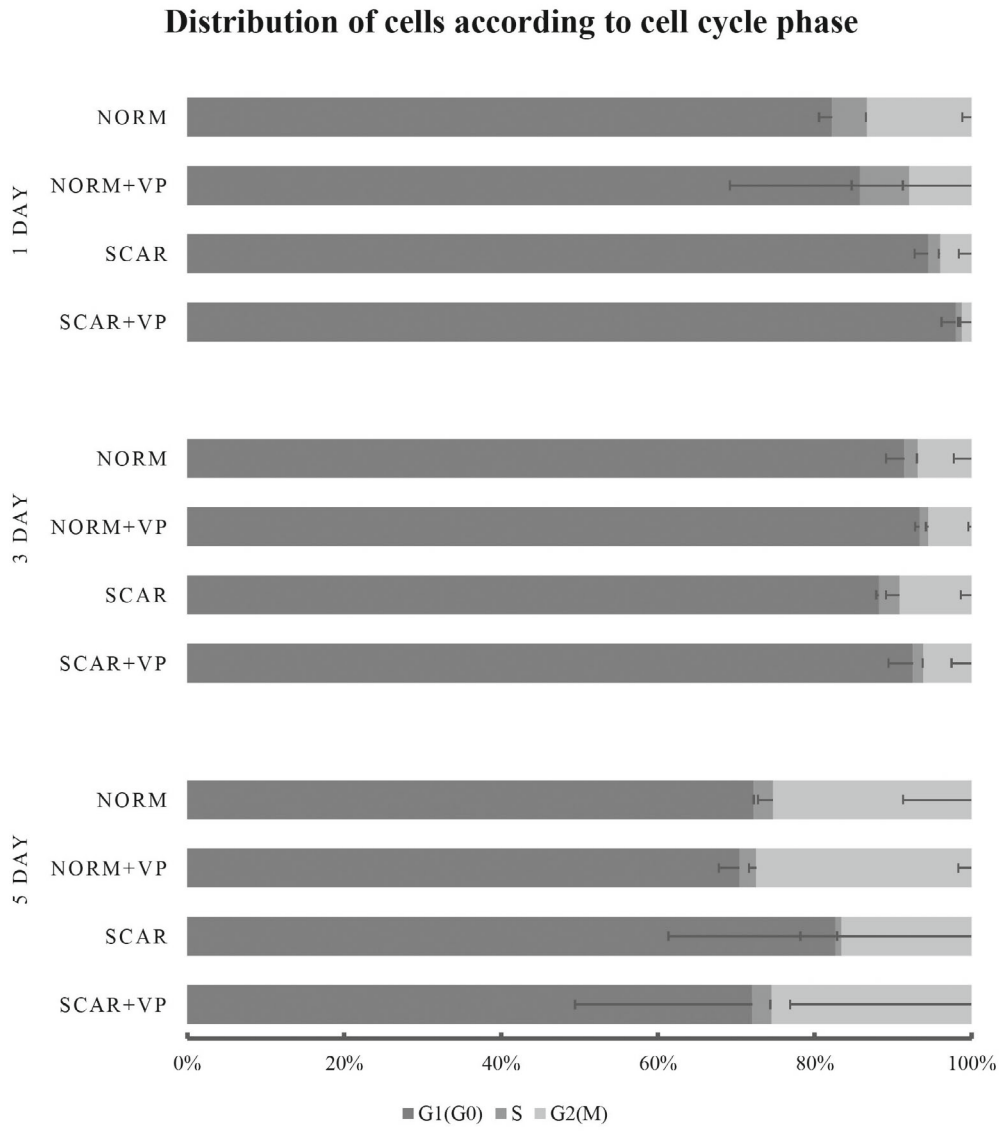


**Fig. 2.** Analysis of cell cycle of normal (norm) and scar-derived (scar) fibroblasts after VP treatment. Data are presented as a mean ± standard deviation.

Considering that the analysis did not reveal any differences in the cell death, but showed differences in proliferation, we decided to analyze of the cell cycle (Fig. 2).

No statistically significant changes in distribution of cells according to the cell cycle phases after treatment with VP were observed. Nevertheless, this diagram allows suggesting that the decrease in proliferation is due to delay in the G1 phase.

**Effect of VP on behaviour of dermal fibroblasts in a collagen gel.** Fibroblasts placed into the collagen gel after just one day form contacts with the collagen fibrils acquiring elongated phenotype typical for this type of cells. At the same time fibroblasts initiate contraction of the gel. Incubation in the presence of 0.1 μg/ml of VP was carried out for 24 h in the half of the prepared gels; culture medium with added DMSO was used as a control. Evaluation of the gel size was estimated 3, 5, and 7 days after treatment (Fig. 3a). Results of the analysis demonstrated that VP initially decreases the degree of gel contraction in both types of investigated fibroblasts. The scar-derived fibroblasts preserved their fibrotic properties during cultivation and contracted gel to a greater degree in comparison with the normal fibroblasts. The analyzed gels visually contained the same number of cells; hence, intensity of contraction was determined by the characteristics of fibroblasts.

Expression of Sm22α, one of the markers of myofibroblasts mediating their contractile capacity, was investigated using immunofluorescent techniques [25-27]. Expression of the elements of the YAP1 signaling pathway was also evaluated, because VP is an inhibitor of this cascade [28, 29] (Fig. 3).

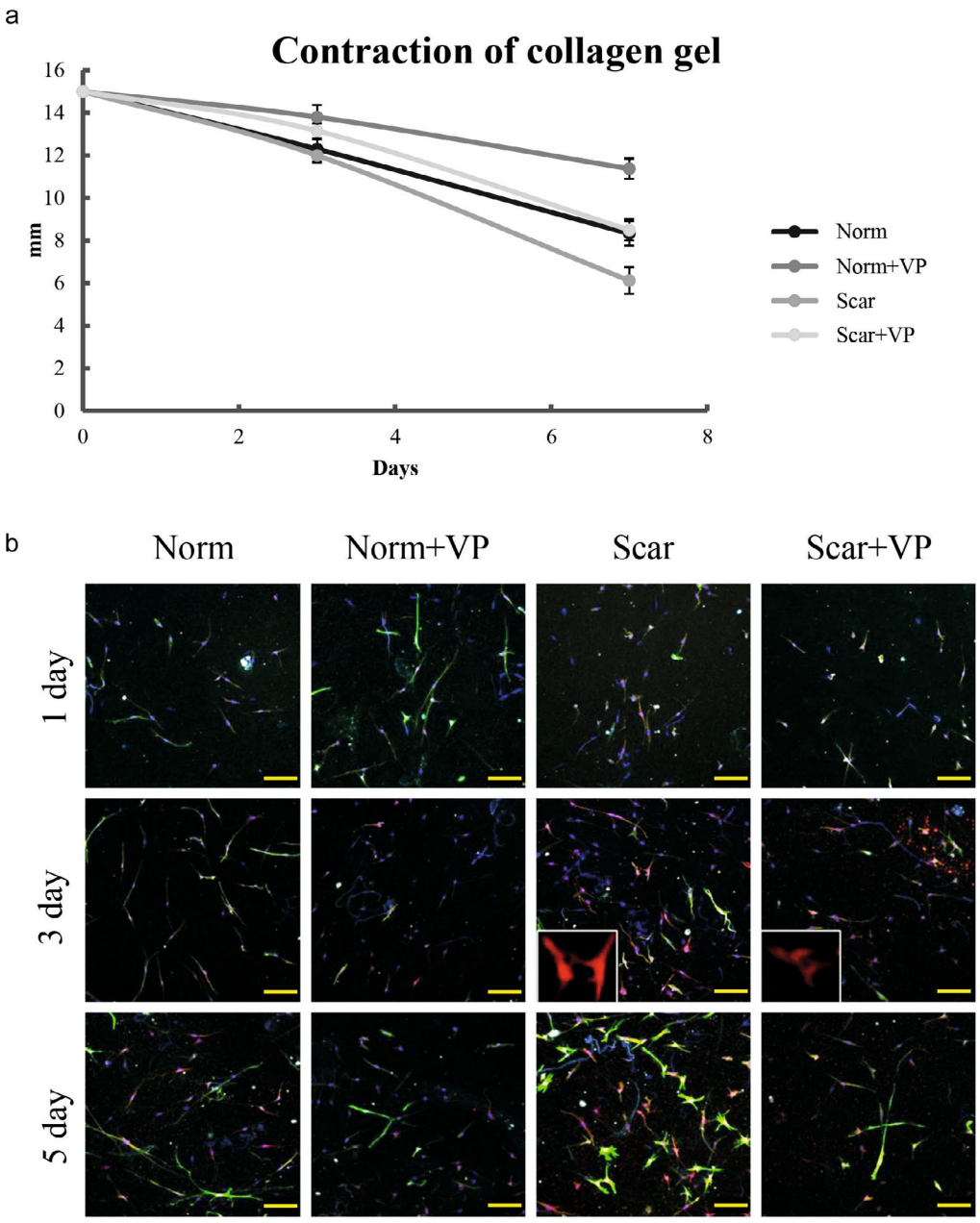


**Fig. 3.** Effect of VP treatment on contractile capacity and phenotypes of different types of fibroblasts (norm and scar) in the collagen gels. a) Dynamics of collagen gels contraction. b) Immunofluorescent identification of Sm22α (green) and YAP1 (red). Cells with cytoplasmic localization of YAP1 are shown in insets at high magnification. Nuclei are stained with DAPI. Confocal microscopy. Scale bar: 100 μm.

The scar-derived fibroblasts contained a larger fraction of Sm22α-positive cells; this difference was most pronounced at the day 5 of cultivation. VP treatment significantly decreased the Sm22α expression in both investigated groups. Expression of YAP1 after exposure to VP also decreased after 3 and 5 day of cultivation. On the day 3 of cultivation, the cells not containing nuclear form of YAP1 were observed in the cultures treated with VP. At the day 5 of cultivation, cells containing nuclear active form of YAP1 were again detected in all cultures (Fig. 3b).

Expression of myofibroblasts markers, proteins of extracellular matrix: collagens type I and III (COL1, COL3) and fibronectin containing extra domain A (EDA-FN), as well as CD26, was evaluated 5 days after exposure of the fibroblasts in collagen gel to VP (Fig. 4). Expression of YAP1 and its paralogue TAZ was evaluated at the same time, because increase of their expression occurs in the course of skin regeneration and during formation of hypertrophic scars, as well as of their typical targets CTGF and CYR61. Analysis of the data obtained with real-time PCR did not reveal

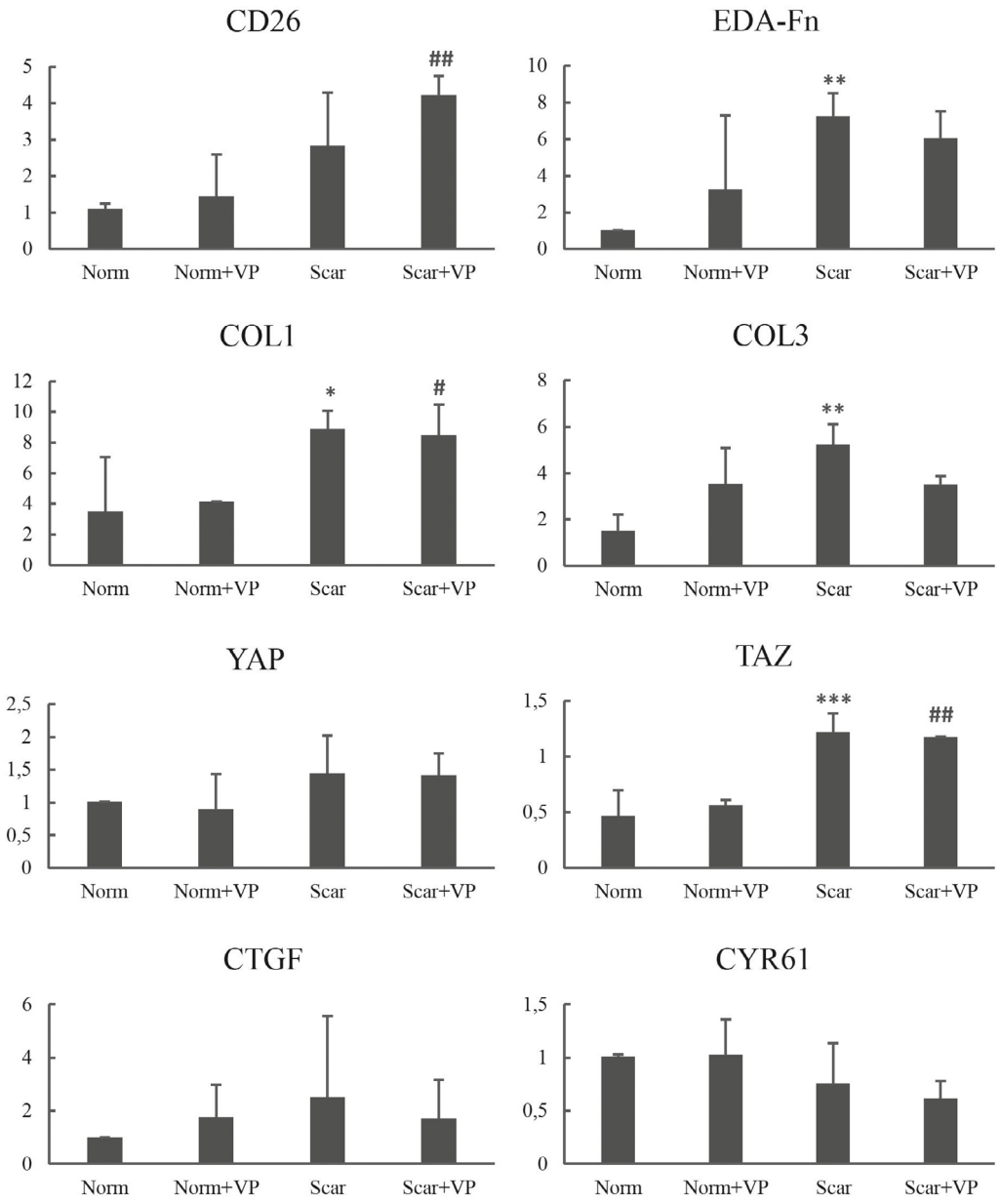


**Fig. 4.** Quantitative PCR analysis of fibrotic markers expressed by different types of fibroblasts (norm and scar) in the collagen gel 5 days after exposure to VP. Data are shown as a mean ± standard deviation. Results were normalized to the level of GAPDH expression. Statistically significant difference of the levels of expression in the scar-derived fibroblasts in comparison with normal fibroblasts: * $p < 0.05$; ** $p < 0.01$; *** $p < 0.001$. Statistically significant difference of the levels of expression in comparison with the 'Norm + VP' group: # $p < 0.05$; ## $p < 0.01$.

any significant differences in the groups of fibroblasts exposed to VP. However, difference between the fibroblasts from normal skin and from scar tissues was statistically significant (Fig. 4).

**Effect of VP on skin morphology in the course of post-traumatic regeneration.** VP was introduced to mice after creation of an artificial splinted wound in composition of a collagen gel or as a solution at the early stages of wound healing. This protocol was based on the previously published data reporting results of a single administration of VP into the wound area [17, 18, 20]. Wounds were imaged every 7 days to assess the rate of their closure (Fig. 5a).

Major number of wounds was closed at the day 14. At the day 22 after surgery the wound area was visually indistinguishable from the normal skin (Fig. 5, a and b). The most pronounced differences in the rate of wound closure were observed at the day 7 after surgery. The wounds in the presence of collagen gel (groups 'Gel' and 'Gel + VP') were closing slower over the first week in comparison with the groups without gel ('Control' and 'VP') (Fig. 5c). At the same time,

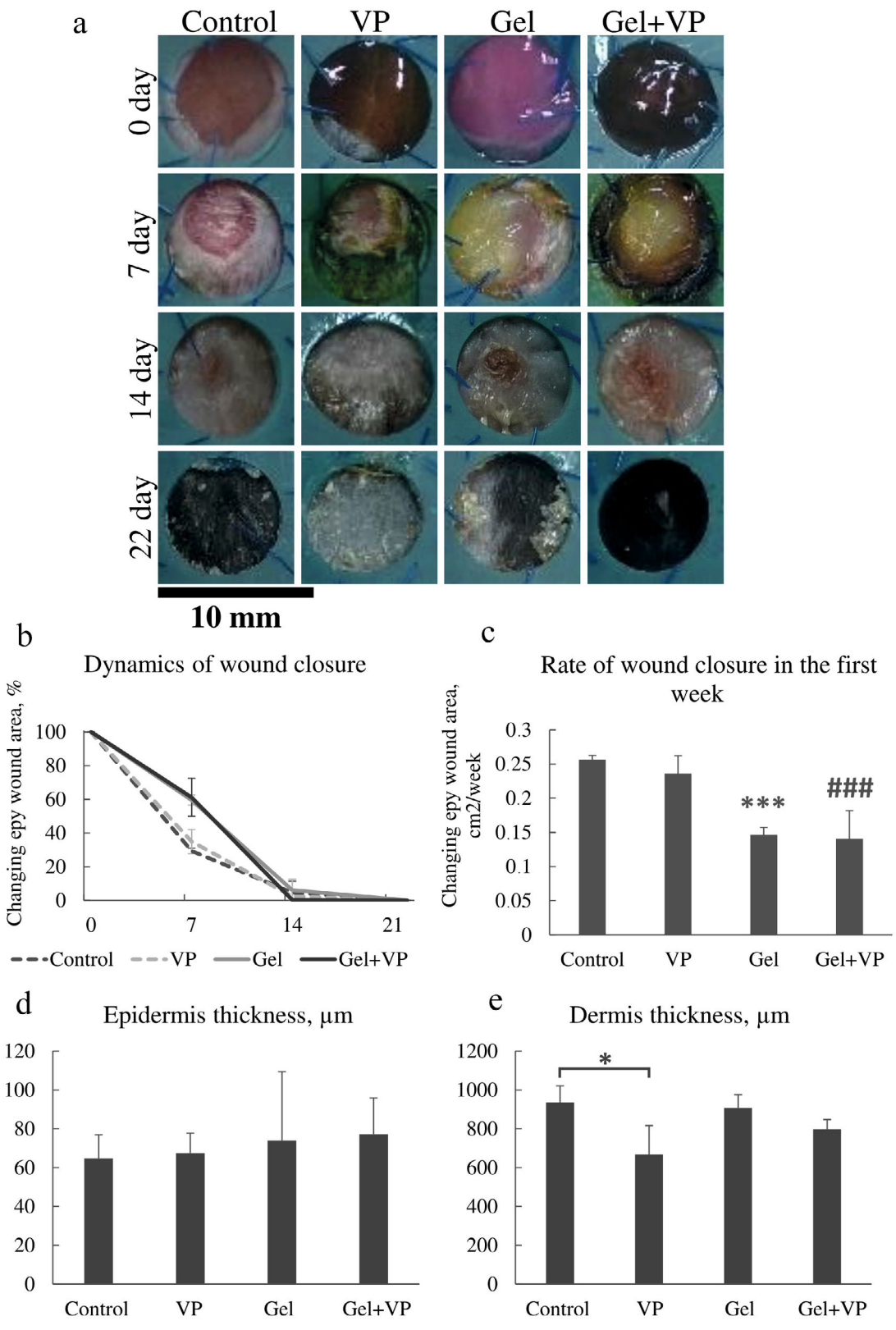


**Fig. 5.** Analysis of dynamics of wound healing based on morphometric parameters. a) Morphology of wounds in different groups at the day 0, 7, 14, and 22 after surgery; b) dynamics of wound closure over the 22-day experiment; c) rate of wound closure in the first week. *** $p < 0.001$ in comparison with control group; ### $p < 0.001$ in comparison with VP group. d) Epidermis thickness in the wound area. e) Dermis thickness in the wound area, * $p < 0.05$. The data are presented as a mean ± standard deviation.

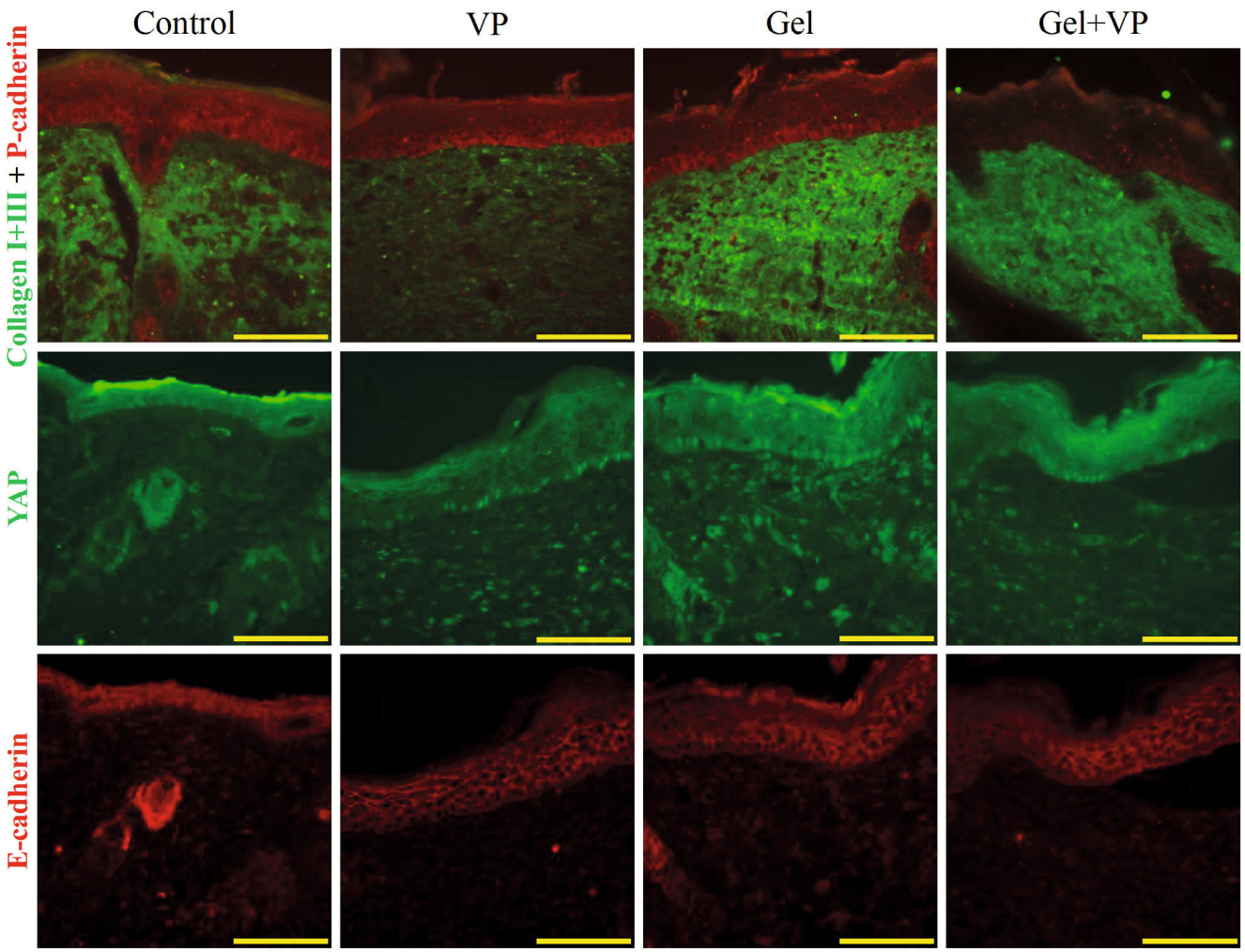


**Fig. 6.** Immunofluorescence detection of wound healing markers (collagens I + III, P-cadherin, E-cadherin, YAP) in the skin section from the wounds at the day 22 after surgery in different groups of mice. Fluorescence microscopy. Scale bar: 100 μm.

there were no differences in the rates of wound healing between the groups with VP exposure ('Gel + VP' and 'VP') and the corresponding groups of mice without VP exposure ('Gel' and 'Control') (Fig. 5, b and c).

Histological examination of skin sections revealed decrease of the dermis thickness in the 'VP' group (Fig. 5e). Epidermis thickness (Fig. 5d) in the wound area was approximately the same in all groups.

Immunofluorescence analysis revealed lower content of the collagens type I and III in the 'VP' group (Fig. 6). Despite the capacity of VP to inhibit the YAP1 signaling [28, 29], the level of active nuclear form of this protein in all dermis samples was the same, as well as in part of the cells of the basal layer of epidermis independent on the presence of VP.

To examine the state of regenerating dermis, analysis of collagen fibers in the histological samples of the skin wounds was performed on the day 22 after surgery with the help of CT-FIRE and CurveAlign algorithms (Fig. 7a). Increase of the length, width, and straightness of individual fibers as well as their alignment relative to each other indicate pronounced fibrosis, which implies slower remodelling process. Significant deviation from the control group characterizes the process of skin regeneration as pathological.

Data obtained with the help of CurveAlign and CT-FIRE were processed using principal component analysis to reduce dimensions. No significant differences in the collagen morphology were revealed between the groups 'Control' and 'VP' after evaluation of all parameters (Fig. 7, b and c). Both the samples from the 'Control" group and from the 'VP' group contained more straightened and longer fibers, which could be typical for the fibrotic stage of normal wound healing [30]. Such samples with more pronounced fibrotic phenotype formed a separate cluster (Fig. 7b; Cluster 1).

Introduction of VP into the collagen gel ('Gel + VP' group) resulted in the increase of width, length, and straightness of the fibers in comparison with the wounds with only collagen gel ('Gel' group, Fig. 7, d and e).

Combining all four groups in one common space of principal coordinates (Fig. 7, f and g) did not demon-

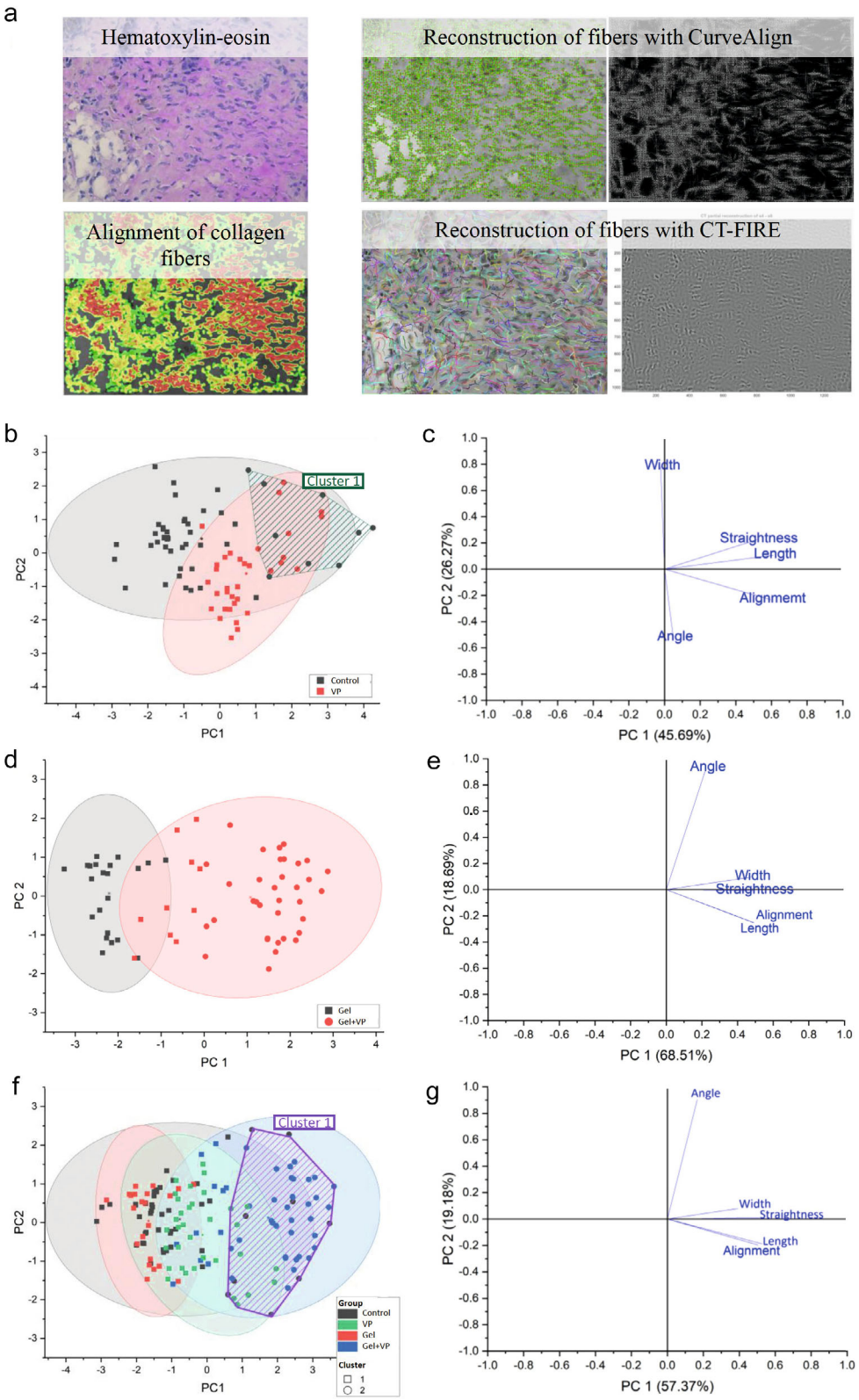


**Fig. 7.** Digital analysis of collagen fibers in histological preparations of mice skin samples obtained 22 days after surgery: a) Visualization of the steps of analysis of collagen fiber structure in histological preparations using heatmaps constructed with the help of CT-FIRE and CurveAlign algorithms. b) Principal component analysis for the 'Control' and 'VP' groups based on the CT-FIRE and CurveAlign data. c) Directions of initial coordinate axes in the principal components space. d) Principal component analysis for the 'Gel' and 'Gel + VP' groups based on the CT-FIRE and CurveAlign data. e) Directions of initial coordinate axes in the principal components space. f) Principal component analysis for all experimental groups based on the CT-FIRE and CurveAlign data. g) Directions of initial coordinate axes in the principal components space.

strate any separations between the groups 'Control', 'VP', and 'Gel', while the group 'Gel + VP' deviates from all other groups. Major part of the observations from the 'Gel + VP' group is located in the separate cluster (Fig. 7f; Cluster 1). Collagen fibers in this cluster are characterized with greater length, width, straightness, and degree of alignment, which could indicate larger extent of fibrotic changes in the dermis.

## DISCUSSIONS

In the course of this study potential effects of VP in combination with collagen gel on the mechanisms of post-traumatic skin regeneration were evaluated.

Preservation of fibrotic properties by the scar-derived fibroblasts during cultivation has been confirmed with immunohistochemical staining (Fig. 3b) and quantitative PCR analysis (Fig. 4), which demonstrate significantly higher expression of the myofibroblast markers in comparison with the control group. The mechanism of VP action in the mouse wounds are commonly associated with elimination of myofibroblasts positive for Engrailed 1 and CD26 from the damage area by inhibiting the YAP/TAZ signaling [18, 20, 29]. It was shown in our *in vitro* experiments that VP does not cause death of the cells, including those isolated from the scar with pronounced fibrotic phenotype. VP decreases proliferation at the first day of cultivation, but the level of proliferation is restored to control levels in the following days (Fig. 1), hence, exposure to VP leads to the elimination of myofibroblasts not by their death, but by altering their of their expression profile from expression of fibrotic markers to the expression profile typical for normal skin.

VP significantly decreases contractile capability of fibroblasts (Fig. 3a). This is associated with the decrease of the fraction of cells positive for expression of the contractile protein Sm22α already at the day 3 after exposure to VP (Fig. 3b).

Exactly at that time the cells not containing active nuclear form of the YAP1 protein were observed. At the day 5 expression profile of the specialized markers of myofibroblasts was analyzed using quantitative PCR analysis (Fig. 4). At this time, we did not observe any statistically significant differences between the groups under exposure to VP and without it in terms of expression of both protein of extracellular matrix and other fibrotic markers, CD26 and YAP/TAZ protein. Activity of the YAP1 signaling was restored, which was manifested by the lack of differences in the expression of its targets CTGF and CYR61. Hence, VP exhibited most pronounced effects on the dermis fibroblasts in culture exactly at the early stages suppressing expression of contractile proteins resulting in the decrease of contraction for up to 7 days, which prolonged its antifibrotic action.

The wound healing in mice is a process significantly different from the process observed in humans [31]. Contraction is more pronounced in the mouse skin, which facilitates closure of even large wounds within a few days. We used splinted wound model in our study to prevent contraction, which makes the process of wound healing in mice closer to the similar process in a human [32]. VP was introduced into a wound either on its own or in composition of a collagen gel. The state of regenerating skin was evaluated on the day 22 at the stage of remodelling in order to obtain detailed characteristics of the process.

At early stages collagen gel slowed down the process of wound closure, however, after the day 14 the damaged area contracted with the same intensity independent on the particular group (Fig. 5). Nuclear YAP1 was detected in the dermis and epidermis at the day 22, which indicated restoration of activity of this signaling cascade (Fig. 6). Addition of VP and collagen gel separately or in combination did not result in the changes of the majority of skin morphological parameters, however, VP introduced separately into the wound decreased thickness of the dermis in regenerating skin (Fig. 5) and intensity of expression of collagen I and III in it (Fig. 6), which indicates its anti-scarring effect [33]. To evaluate the manifestations of fibrosis in the course of skin regeneration modern methods of computer-assisted analysis of extracellular matrix morphology were used [23, 24]. Introduction of VP in the composition of collagen gel ('Gel + VP' group) resulted in formation of fibers with larger length, width, and straightness (Fig. 7, b and c). Formation of such fibers indicates fibrotic direction of the wound healing process [34]. Furthermore, analysis of the parameters characterizing morphology of collagen fibers did not reveal any statistically significant differences between the groups 'VP' and 'Gel' and the 'Control' group. Although application of VP and collagen gel do not change morphology of collagen fibers, their use, which is important, does not lead to activation of fibrosis. Hence, despite the positive effect of VP administration, its combination with collagen gel affected regeneration process in a negative way. Unlike in our study, success of VP administration in composition of specialized carriers was observed only in the cases when the carriers comprised not a single layer covering the wound area, but microparticles containing VP [12, 14, 15]. The result observed in our study could be explained by several mechanisms underlying the effects of collagen gel and VP on wound healing. VP modulated behavior of fibroblasts preventing contraction of the collagen gel (Fig. 3a) and decreasing expression of fibrotic markers (Fig. 4). Collagen gel, in turn, stimulates more intensive

formation of granulation tissue, which accelerates regeneration process [35, 36]. It is likely that VP inhibited formation of the pool of myofibroblasts, which, in turn, slowed down the stage of proliferation and remodelling and caused the observed manifestations of fibrosis.

## CONCLUSIONS

Development of tissue engineering constructs stimulating wound healing, but not resulting in scar formation is very important for the patients with burns and other pathologies. VP is one of the most promising antifibrotic preparations, hence, the possibility of its use in composition of therapeutics stimulating regeneration processes has been considered [18, 20, 29]. Collagen gels are also used for skin wound closing [6-8]. It was shown in our study that combined application of the collagen gel and VP enhanced fibrosis during wound healing. Hence, the current way of VP administration into the wound does not facilitate regeneration; that is why the possible carriers of VP for wound healing require further investigation. Application of the constructs containing dermal fibroblasts and epidermal keratinocytes stimulated skin regeneration more effectively in comparison with application of empty carriers [37], hence, addition of cellular component could help to optimize properties of the gel with preserving its regenerative potential. As was shown in our *in vitro* experiments, VP did not cause cell death, but prevented fibrotic changes in the cellular component in the composition of the collagen gel. Hence, dermal fibroblasts inside the carriers could preserve their normal phenotype after exposure to VP and after transplantation to the area of skin damage. This possibility should be examined in future studies, as well as optimization of the composition of specialized carrier.

**Acknowledgments.** Cell lines used in the study were provided by the Collection of Cell Cultures of the Center for Collective Usage of the Institute of Developmental Biology, Russian Academy of Sciences. Equipment from the Center for Collective Usage of the Institute of Developmental Biology, Russian Academy of Sciences, was used in the study.

**Contributions.** O.S.R., A.D.S., and K.E.P. were responsible for conducting *in vitro* experiments; S.A.D. performed quantitative PCR analysis; O.S.R., A.D.S., Ch.O.L., and K.E.P. performed experiments with laboratory animals; Ch.O.L. performed bioinformatics analysis of distribution of extracellular matrix fibers in the wound area; O.S.R., V.E.A., and K.E.P. development of the study design; O.S.R., Ch.O.L., and K.E.P. preparation of the text of the paper; V.E.A. editing text of the paper.

**Funding.** The study was financially supported by the Russian Science Foundation (project no. 21-74-30015, https://rscf.ru/en/project/21-74-30015/).

**Ethics declarations.** All procedures performed in studies involving human participants were in accordance with the ethical standards of the institutional and/or national research committee and with the 1964 Helsinki declaration and its later amendments or comparable ethical standards. All applicable international, national, and/or institutional guidelines for the care and use of animals were followed. The authors of this work declare that they have no conflicts of interest.

## REFERENCES

1. Cañedo-Dorantes, L., and Cañedo-Ayala, M. (2019) Skin acute wound healing: a comprehensive review, *Int. J. Inflamm.*, **2019**, 3706315, doi: 10.1155/2019/3706315.
2. Xue, M., and Jackson, C. J. (2015) Extracellular matrix reorganization during wound healing and its impact on abnormal scarring, *Adv. Wound Care*, **4**, 119-136, doi: 10.1089/wound.2013.0485.
3. Karppinen, S.-M., Heljasvaara, R., Gullberg, D., Tasanen, K., and Pihlajaniemi, T. (2019) Toward understanding scarless skin wound healing and pathological scarring, *F1000Res.*, **8**, 787, doi: 10.12688/f1000research.18293.1.
4. Tomasek, J. J., Gabbiani, G., Hinz, B., Chaponnier, C., and Brown, R. A. (2002) Myofibroblasts and mechano-regulation of connective tissue remodelling, *Nat. Rev. Mol. Cell Biol.*, **3**, 349-363, doi: 10.1038/nrm809.
5. Eudy, M., Eudy, C. L., and Roy, S. (2021) Apligraf as an alternative to skin grafting in the pediatric population, *Cureus*, **13**, e16226, doi: 10.7759/cureus.16226.
6. Dibbs, R. P., Depani, M., and Thornton, J. F. (2022) Technical refinements with the use of biologic healing agents, *Semin. Plast. Surg.*, **36**, 008-016, doi: 10.1055/s-0042-1742749.
7. El Masry, M. S., Chaffee, S., Das Ghatak, P., Mathew-Steiner, S. S., Das, A., Higuita-Castro, N., Roy, S., Anani, R. A., and Sen, C. K. (2019) Stabilized collagen matrix dressing improves wound macrophage function and epithelialization, *FASEB J.*, **33**, 2144-2155, doi: 10.1096/fj.201800352R.
8. Parenteau-Bareil, R., Gauvin, R., and Berthod, F. (2010) Collagen-based biomaterials for tissue engineering applications, *Materials*, **3**, 1863-1887, doi: 10.3390/ma3031863.
9. Mouw, J. K., Ou, G., and Weaver, V. M. (2014) Extracellular matrix assembly: a multiscale deconstruction, *Nat. Rev. Mol. Cell Biol.*, **15**, 771-785, doi: 10.1038/nrm3902.
10. Hynes, R. O. (2014) Stretching the boundaries of extracellular matrix research, *Nat. Rev. Mol. Cell Biol.*, **15**, 761-763, doi: 10.1038/nrm3908.

11. Mathew-Steiner, S. S., Roy, S., and Sen, C. K. (2021) Collagen in wound healing, *Bioengineering*, **8**, 63, doi: 10.3390/bioengineering8050063.
12. Zhang, Y., Wang, Y., Li, Y., Yang, Y., Jin, M., Lin, X., Zhuang, Z., Guo, K., Zhang, T., and Tan, W. (2023) Application of collagen-based hydrogel in skin wound healing, *Gels*, **9**, 185, doi: 10.3390/gels9030185.
13. Potter, D. A., Veitch, D., and Johnston, G. A. (2019) Scarring and wound healing, *Br. J. Hosp. Med. Lond. Engl.*, **80**, C166-C171, doi: 10.12968/hmed.2019.80.11.C166.
14. Chen, K., Liu, Y., Liu, X., Guo, Y., Liu, J., Ding, J., Zhang, Z., Ni, X., and Chen, Y. (2023) Hyaluronic acid-modified and verteporfin-loaded polylactic acid nanogels promote scarless wound healing by accelerating wound re-epithelialization and controlling scar formation, *J. Nanobiotechnol.*, **21**, 241, doi: 10.1186/s12951-023-02014-x.
15. Wei, C., You, C., Zhou, L., Liu, H., Zhou, S., Wang, X., and Guo, R. (2023) Antimicrobial hydrogel microneedle loading verteporfin promotes skin regeneration by blocking mechanotransduction signaling, *Chem. Eng. J.*, **472**, 144866, doi: 10.1016/j.cej.2023.144866.
16. Zhang, C., Yang, D., Wang, T.-B., Nie, X., Chen, G., Wang, L.-H., You, Y.-Z., and Wang, Q. (2022) Biodegradable hydrogels with photodynamic antibacterial activity promote wound healing and mitigate scar formation, *Biomater. Sci.*, **11**, 288-297, doi: 10.1039/D2BM01493A.
17. Zhang, Y., Wang, S., Yang, Y., Zhao, S., You, J., Wang, J., Cai, J., Wang, H., Wang, J., Zhang, W., Yu, J., Han, C., Zhang, Y., and Gu, Z. (2023) Scarless wound healing programmed by core-shell microneedles, *Nat. Commun.*, **14**, 3431, doi: 10.1038/s41467-023-39129-6.
18. Mascharak, S., Talbott, H. E., Januszyk, M., Griffin, M., Chen, K., Davitt, M. F., Demeter, J., Henn, D., Bonham, C. A., Foster, D. S., Mooney, N., Cheng, R., Jackson, P. K., Wan, D. C., Gurtner, G. C., and Longaker, M. T. (2022) Multi-Omic analysis reveals divergent molecular events in scarring and regenerative wound healing, *Cell Stem Cell*, **29**, 315-327.e6, doi: 10.1016/j.stem.2021.12.011.
19. Lee, M.-J., Byun, M. R., Furutani-Seiki, M., Hong, J.-H., and Jung, H.-S. (2014) YAP and TAZ regulate skin wound healing, *J. Invest. Dermatol.*, **134**, 518-525, doi: 10.1038/jid.2013.339.
20. Mascharak, S., desJardins-Park, H. E., Davitt, M. F., Griffin, M., Borrelli, M. R., Moore, A. L., Chen, K., Duoto, B., Chinta, M., Foster, D. S., Shen, A. H., Januszyk, M., Kwon, S. H., Wernig, G., Wan, D. C., Lorenz, H. P., Gurtner, G. C., and Longaker, M. T. (2021) Preventing engrailed-1 activation in fibroblasts yields wound regeneration without scarring, *Science*, **372**, eaba2374, doi: 10.1126/science.aba2374.
21. International Guiding Principles for Biomedical Research Involving Animals (1985) In *The Development of Science-based Guidelines for Laboratory Animal Care: Proceedings of the November 2003 International Workshop*; National Academies Press (US), 2004.
22. European Convention for the Protection of Vertebrate Animals Used for Experimental and Other Scientific Purposes, URL: https://www.ecolex.org/details/treaty/european-convention-for-the-protection-of-vertebrate-animals-used-for-experimental-and-other-scientific-purposes-tre-001042/.
23. Bredfeldt, J. S., Liu, Y., Pehlke, C. A., Conklin, M. W., Szulczewski, J. M., Inman, D. R., Keely, P. J., Nowak, R. D., Mackie, T. R., and Eliceiri, K. W. (2014) Computational segmentation of collagen fibers from second-harmonic generation images of breast cancer, *J. Biomed. Opt.*, **19**, 16007, doi: 10.1117/1.JBO.19.1.016007.
24. Liu, Y., Keikhosravi, A., Mehta, G. S., Drifka, C. R., and Eliceiri, K. W. (2017) Methods for quantifying fibrillar collagen alignment, *Methods Mol. Biol.*, **1627**, 429-451, doi: 10.1007/978-1-4939-7113-8_28.
25. Mussbacher, M., Salzmann, M., Brostjan, C., Hoesel, B., Schoergenhofer, C., Datler, H., Hohensinner, P., Basílio, J., Petzelbauer, P., Assinger, A., and Schmid, J. A. (2019) Cell type-specific roles of NF-κB linking inflammation and thrombosis, *Front. Immunol.*, **10**, 85, doi: 10.3389/fimmu.2019.00085.
26. Wnuk, D., Lasota, S., Paw, M., Madeja, Z., and Michalik, M. (2020) Asthma-derived fibroblast to myofibroblast transition is enhanced in comparison to fibroblasts derived from non-asthmatic patients in 3D *in vitro* culture due to Smad2/3 signalling, *Acta Biochim. Pol.*, **67**, 441-448, doi: 10.18388/abp.2020_5412.
27. Shin, D., and Minn, K. W. (2004) The effect of myofibroblast on contracture of hypertrophic scar, *Plast. Reconstr. Surg.*, **113**, 633-640, doi: 10.1097/01.PRS.0000101530.33096.5B.
28. Wang, C., Zhu, X., Feng, W., Yu, Y., Jeong, K., Guo, W., Lu, Y., and Mills, G. B. (2016) Verteporfin inhibits YAP function through Up-regulating 14-3-3σ sequestering YAP in the cytoplasm, *Am. J. Cancer Res.*, **6**, 27-37.
29. Shi-wen, X., Racanelli, M., Ali, A., Simon, A., Quesnel, K., Stratton, R. J., and Leask, A. (2021) Verteporfin inhibits the persistent fibrotic phenotype of lesional scleroderma dermal fibroblasts, *J. Cell Commun. Signal.*, **15**, 71-80, doi: 10.1007/s12079-020-00596-x.
30. El Ayadi, A., Jay, J. W., and Prasai, A. (2020) Current approaches targeting the wound healing phases to attenuate fibrosis and scarring, *Int. J. Mol. Sci.*, **21**, 1105, doi: 10.3390/ijms21031105.
31. Zlobina, K., Malekos, E., Chen, H., and Gomez, M. (2023) Robust classification of wound healing stages in both mice and humans for acute and burn wounds based on transcriptomic data, *BMC Bioinformatics*, **24**, 166, doi: 10.1186/s12859-023-05295-z.
32. Galiano, R. D., Michaels, J., Dobryansky, M., Levine, J. P., and Gurtner, G. C. (2004) Quantitative and reproducible murine model of excisional wound healing,

*Wound Repair Regen.*, **12**, 485-492, doi: 10.1111/j.1067-1927.2004.12404.x.

33. Ud-Din, S., Foden, P., Stocking, K., Mazhari, M., Al-Habba, S., Baguneid, M., McGeorge, D., and Bayat, A. (2019) Objective assessment of dermal fibrosis in cutaneous scarring, using optical coherence tomography, high-frequency ultrasound and immunohistomorphometry of human skin, *Br. J. Dermatol.*, **181**, 722-732, doi: 10.1111/bjd.17739.
34. Henn, D., Chen, K., Fehlmann, T., Trotsyuk, A. A., Sivaraj, D., Maan, Z. N., Bonham, C. A., Barrera, J. A., Mays, C. J., Greco, A. H., Moortgat Illouz, S. E., Lin, J. Q., Steele, S. R., Foster, D. S., Padmanabhan, J., Momeni, A., Nguyen, D., Wan, D. C., Kneser, U., Januszyk, M., Keller, A., Longaker, M. T., and Gurtner, G. C. (2021) Xenogeneic skin transplantation promotes angiogenesis and tissue regeneration through activated $Trem^{2+}$ macrophages, *Sci. Adv.*, **7**, eabi4528, doi: 10.1126/sciadv.abi4528.
35. Brett, D. A. (2008) Review of collagen and collagen-based wound dressings, *Wounds Compend. Clin. Res. Pract.*, **20**, 347-356.
36. Ge, B., Wang, H., Li, J., Liu, H., Yin, Y., Zhang, N., and Qin, S. (2020) Comprehensive assessment of Nile tilapia skin (Oreochromis Niloticus) collagen hydrogels for wound dressings, *Mar. Drugs*, **18**, 178, doi: 10.3390/md18040178.
37. Chermnykh, E. S., Kiseleva, E. V., Rogovaya, O. S., Rippa, A. L., Vasiliev, A. V., and Vorotelyak, E. A. (2018) Tissue-engineered biological dressing accelerates skin wound healing in mice via formation of provisional connective tissue, *Histol. Histopathol.*, **33**, 1189-1199, doi: 10.14670/HH-18-006.